The invariant chain transports TNF family member CD70 to MHC class II compartments in dendritic cells

Wilbert Zwart[1], Victor Peperzak[2,*], Evert de Vries[2,*], Anna M. Keller[2,*,‡], Gerda van der Horst[2], Elise A. M. Veraar[2], Ulf Geumann[2], Hans Janssen[1], Lennert Janssen[1], Shalin H. Naik[2], Jacques Neefjes[1] and Jannie Borst[2,§]

[1]Division of Cell Biology and [2]Division of Immunology, The Netherlands Cancer Institute, 1066 CX Amsterdam, The Netherlands

*These authors contributed equally to this work

‡Present address: London Research Institute, Cancer Research UK, London WC2A 3PX, UK

§Author for correspondence (j.borst@nki.nl)

Accepted 1 July 2010
Journal of Cell Science 123, 3817-3827

doi:10.1242/jcs.068510

Summary

CD70 is a TNF-related transmembrane molecule expressed by mature dendritic cells (DCs), which present antigens to T cells via major histocompatibility complex (MHC) molecules. In DCs, CD70 localizes with MHC class II molecules in late endosomal vesicles, known as MHC class II compartments (MIICs). MIICs are transported to the immune synapse when a DC contacts an antigen-specific $CD4^+$ T cell. Consequently, MHC class II and CD70 are simultaneously exposed to the T cell. Thereby, T-cell activation via the antigen receptor and CD70-mediated co-stimulation are synchronized, apparently to optimize the proliferative response. We report here that the invariant chain (Ii), a chaperone known to transport MHC class II to MIICs, performs a similar function for CD70. CD70 was found to travel by default to the plasma membrane, whereas Ii coexpression directed it to late endosomes and/or lysosomes. In cells containing the MHC class II presentation pathway, CD70 localized to MIICs. This localization relied on Ii, since transport of CD70 from the Golgi to MIICs was impeded in Ii-deficient DCs. Biophysical and biochemical studies revealed that CD70 and Ii participate in an MHC-class-II-independent complex. Thus, Ii supports transport of both MHC class II and CD70 to MIICs and thereby coordinates their delivery to $CD4^+$ T cells.

Key words: CD70, Invariant chain, MHC class II, Intracellular transport, Dendritic cells

Introduction

Dendritic cells (DCs) are specialized antigen-presenting cells that can initiate clonal expansion of antigen-specific T cells and drive their differentiation into effector cells. To this end, DCs first need to mature, which occurs in response to pathogens that trigger Toll-like receptors (TLR). This optimizes the capacity of DCs to present antigens in major histocompatibility complex (MHC) molecules and thus enables them to trigger the T-cell antigen receptor (TCR), which is essential for initiation of the T-cell response. However, the T cell also requires so-called co-stimulatory signals for an optimal response, which the DC can deliver upon its maturation (Steinman et al., 2003). Important co-stimulatory ligands expressed on mature DCs are the immunoglobulin family members CD80 and CD86, as well as the TNF family member CD70 (Goodwin et al., 1993; Tesselaar et al., 1997). On the T-cell side, these ligands bind respectively to CD28 and CD27, two transmembrane receptors that enable clonal expansion of $CD4^+$ and $CD8^+$ T cells by supporting cell division and survival. Co-stimulation by CD27 and CD70 additionally promotes development of $CD8^+$ T-cell helper- and memory programming functions in $CD4^+$ T cells (Hendriks et al., 2003; Soares et al., 2007; Xiao et al., 2008).

CD70 is absent from resting cells and is transiently expressed at the cell surface of B cells and conventional DCs upon immune activation (Tesselaar et al., 2003a; Hendriks et al., 2005). Strict control of CD70 expression is required to maintain T cell and B cell homeostasis, as demonstrated by the phenotype of transgenic mice with constitutive CD70 expression on B cells or DCs (Arens et al., 2001; Keller et al., 2008). Chronic stimulation of CD27 in these mice resulted in seemingly spontaneous conversion of naive T cells into effector cells, which culminated in a lethal combined T- and B-cell immunodeficiency (Tesselaar et al., 2003b). Transgenic CD70 expression on otherwise immature DCs also broke immunological tolerance, which implies a risk for autoimmunity (Keller et al., 2008). Strict control of CD70 expression apparently ensures that the pro-survival input through CD27 signaling is limited and occurs specifically upon immune activation.

In DCs, CD70 expression is regulated by the selective transcription of CD70 mRNA in response to TLR and/or CD40 signaling (Tesselaar et al., 2003a; Sanchez et al., 2007). We have shown that CD70 is also subject to specialized intracellular trafficking. In maturing DCs, newly synthesized CD70 is transported to MHC class II compartments (MIICs) (Keller et al., 2007). These are late endosomal and/or lysosomal compartments that, in professional antigen-presenting cells, contain MHC class II molecules (Neefjes et al., 1990; Peters et al., 1991). In MIICs, MHC class II is loaded with antigenic peptides derived from extracellular sources (Rocha and Neefjes, 2008). MIICs are essentially secretory lysosomes (Wubbolts et al., 1996) that upon DC activation can transform into tubular structures (Boes et al., 2002; Kleijmeer et al., 2001). We have observed that MIICs moved toward the immune synapse that is formed when a DC makes contact with an antigen-specific $CD4^+$ T cell and simultaneously delivered CD70 and MHC class II to the plasma membrane of the DC at the immune synapse (Keller et al., 2007). We propose that this process serves to spatially and temporally coordinate both antigen presentation and co-stimulation.

We report here that the specific routing of CD70 to MIICs is dictated by Ii (also known as CD74). Ii is widely known as the

obligate chaperone of MHC class II molecules (Cresswell, 1994). Ii pairs with MHC class II in the ER and directs it to MIICs by virtue of unique sorting signals in its cytoplasmic tail (Bakke and Dobberstein, 1990; Lotteau et al., 1990; Odorizzi et al., 1994). In MIICs, Ii is degraded by resident proteolytic enzymes and MHC class II is freed to bind antigenic peptides (Cresswell, 1994). By determining the transport of MHC class II molecules, Ii directs both MHC class II loading with antigenic peptides and its delivery to $CD4^+$ T cells (Bikoff et al., 1993; Viville et al., 1993). We here describe a novel function for Ii in showing that it escorts CD70 to MIICs. We demonstrate that CD70 and Ii form an MHC class II-independent complex in the ER. In DCs that are genetically deficient for Ii, CD70 can exit the ER, but fails to travel from the Golgi to MIICs, indicating that Ii performs a critical role for CD70 routing to MIIC. Ii therefore performs a dual function: it directs transport of CD70 as well as MHC class II to MIICs and thereby allows their simultaneous delivery to the immunological synapse that is formed between a DC and an antigen-specific $CD4^+$ T cell. In this way, T-cell activation via the TCR and T-cell co-stimulation via CD27 are coordinated in time and space.

Results

Ii directs CD70 to late endosomes and/or lysosomes in cells that lack the MHC class II presentation machinery

We previously observed that CD70 travels by default to the plasma membrane in human HeLa cervix carcinoma cells that do not express the MHC class II antigen presentation machinery. However, CD70 was directed towards late endosomes and/or lysosomes when CIITA was coexpressed (Keller et al., 2007). CIITA is a master transcriptional regulator that directs the expression of a multitude of proteins that are characteristic of professional antigen-presenting cells, including Ii (Chang and Flavell, 1995), which we tested for its potential involvement in CD70 transport. Both in human and mouse, Ii occurs in several isoforms that arise from alternative RNA splicing and alternative translation initiation (Strubin et al., 1986; O'Sullivan et al., 1987). For human Ii expression, we used a construct encoding the p33 Ii isoform (hIi-p33) that was previously validated for human MHC class II chaperone function (Nijenhuis and Neefjes, 1994) (see supplementary material Table S1 for sequence). When murine (m)CD70 was expressed alone in HeLa cells, most of the mCD70 molecules were present at the plasma membrane and absent from late endosomes and/or lysomes, as marked by CD63 (Fig. 1A). However, when hIi-p33 was coexpressed with CD70, a large proportion of mCD70 molecules localized, with hIi-p33, in intracellular compartments that were positive for CD63 (Fig. 1A). The re-routing of mCD70 to CD63-containing compartments by hIi-p33 can be further appreciated in the scatter plot analysis of the same images (Fig. 1B). mCD70 (red) and CD63 (green) only marginally colocalized in the absence of hIi-p33, as indicated by a separation of the red and green fluorescence signals along the horizontal and vertical axis of the scatter plot. In the presence of hIi-p33, however, the majority of the mCD70 signals aligned with the CD63 signals along the diagonal axis, indicating colocalization. Both CD63 and CD70 also colocalized with hIi-p33 (blue). Human (h)CD70 also relocated to a significant extent to CD63-positive compartments in HeLa cells upon coexpression of hIi-p33, as demonstrated using confocal laser scanning microscopy (CLSM; supplementary material Fig. S1A) and associated scatter plot analysis (supplementary material Fig. S1B). From these findings, we conclude that Ii redirects CD70 from the default transport route and targets it to late endosomes and/or lysosomes instead.

In cells endowed with the MHC class II presentation pathway, CD70 and Ii colocalize in MIICs

Next, the human melanoma cell line Mel JuSo was employed as model cell line, because it expresses all components of the MHC class II antigen presentation pathway (Pieters et al., 1991). Upon expression in Mel JuSo cells, a fusion protein of mCD70 and monomeric red fluorescent protein (mRFP) localized to the plasma membrane, but another fraction localized intracellularly. This intracellular pool of mCD70–mRFP partially colocalized with endogenous Ii in CD63-positive vesicles (Fig. 2A) as quantified by scatter plot analysis (supplementary material Fig. S2). Unmodified

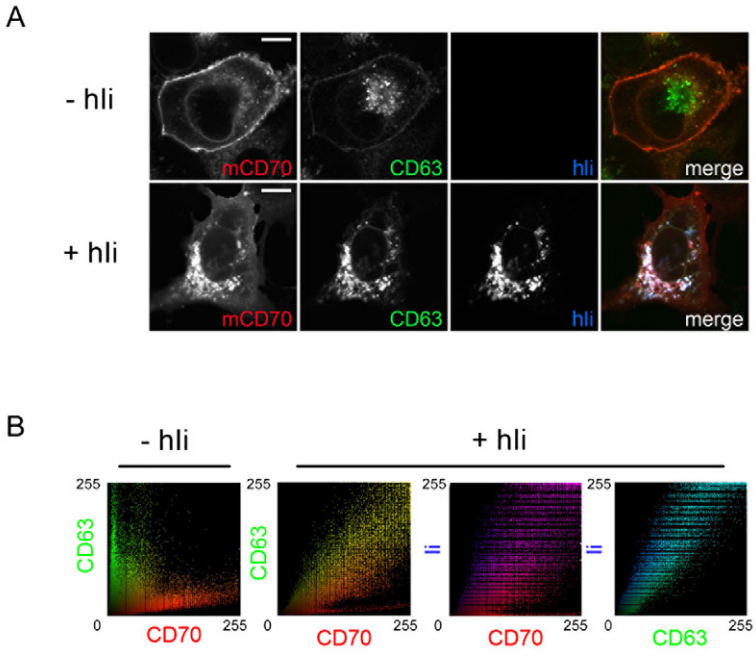

Fig. 1. Localization of CD70 in HeLa cells that lack the MHC class II antigen presentation pathway. (**A**) HeLa cells were transfected to express murine (m)CD70 without (top panel) or with (bottom panel) human (h)Ii, fixed, permeabilized and stained sequentially with anti-CD63–FITC (green), rat anti-mCD70 (FR70) and goat anti-rat Ig–Alexa Fluor 568 (red), mouse anti-human Ii (Bu45) and goat anti-mouse Ig-Alexa Fluor 633 (far red, shown as blue) and examined by CLSM. The merged images show signals from all three channels and colocalization of mCD70, CD63 and hIi appears white. Scale bars: 10 µm. Images are representative of data obtained in two independent experiments (n>20). (**B**) Scatter plot analysis of CD63, CD70 and Ii colocalization in HeLa cells. Images from A were analyzed using the intensity correlation analysis function of the WCIF plugin of ImageJ (www.uhnresearch.ca/wcif), where the signal intensity of each channel was related to the other channels and plotted in a 2D graph.

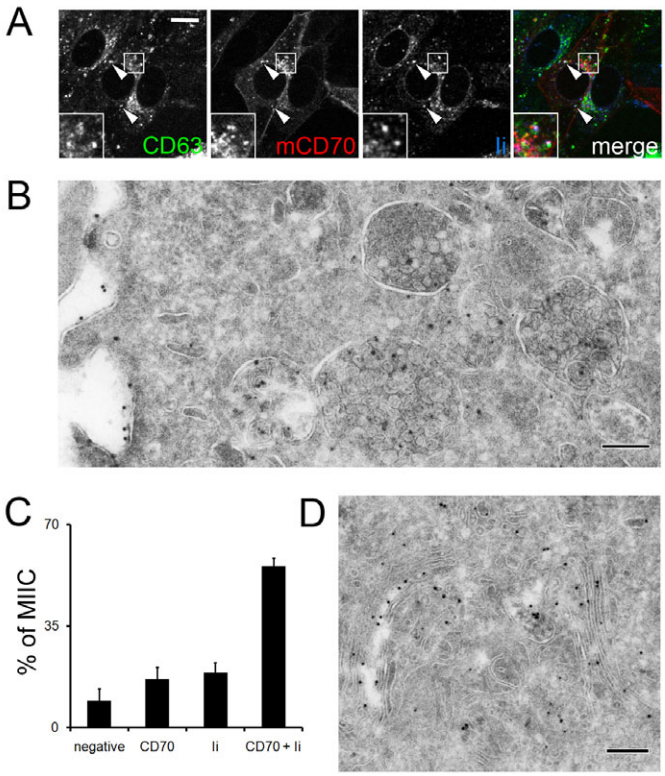

Fig. 2. Localization of CD70 in Mel JuSo cells that have the MHC class II antigen presentation pathway. (**A**) Mel JuSo cells were transfected to express mCD70–mRFP (red), fixed, permeabilized and stained sequentially with mouse anti-human Ii (Bu45) and goat anti-mouse Ig–Alexa Fluor 647 (far red, shown as blue) and with anti-CD63–FITC (green) and examined by CLSM. The merged image shows signals from all three channels and colocalization of mCD70, CD63 and Ii appears white (arrows). Scale bar: 10 µm. Inset shows an enlarged view of the boxed region. Images are representative of two independent experiments (n>30). See supplementary material Fig. S2 for pixel analysis of these images. (**B-D**) Mel JuSo cells, stably expressing untagged mCD70 were fixed and processed for immuno-EM. Sections were stained for mCD70 with FR70 mAb (large gold particles) and for endogenous human Ii with ICN1 polyclonal (small gold particles). MIICs (B) and Golgi structures (D) were analyzed. Colocalization of CD70 and Ii within morphologically defined MIICs was quantified (C) as the percentage of MIICs without CD70 or Ii (negative), with Ii or CD70 only, or with CD70 and Ii. Data are from two independent experiments (n>30). Scale bars: 200 nm (B), 250 nm (C). See supplementary material Fig. S3B for further clarification of B.

human CD70 was similarly distributed with endogenous Ii in CD63-containing compartments (supplementary material Fig. S3A).

To examine the subcellular localization of CD70 and endogenous Ii in more detail, immuno-EM was performed on Mel JuSo cells stably expressing unmodified mCD70. The images revealed the characteristic morphology of MIICs, which is essentially a late endosomal multivesicular body (Peters et al., 1991) (Fig. 2B). Immuno-EM confirmed the CLSM analysis by revealing that mCD70 resided at the plasma membrane, and in addition colocalized with endogenous Ii in MIICs (Fig. 2B). The images showed that mCD70 and Ii were enriched on the internal vesicles of MIICs. Ii was labeled with an antibody to its cytoplasmic tail that detects both intact Ii and lumenally degraded forms and its localization was in agreement with previously published data (Peters et al., 1995). As internal controls, the nucleus or mitochondria did not show labeling for either mCD70 or Ii (Fig. 2B and data not shown). Further detailed analysis is provided in supplementary material Fig. S3B.

Quantification of the immuno-EM data indicated that most MIICs in Mel JuSo cells contained both mCD70 and Ii (Fig. 2C). Detection of either molecule by immuno-EM has a sensitivity threshold, which may explain why some single positive compartments were observed (Fig. 2C). CD70 was also detected in the Golgi (Fig. 2D), as noted before (Keller et al., 2007), explaining the only partial colocalization of the vesicular intracellular CD70 pool with CD63 (Fig. 2A). These data indicate that CD70, in cells with a functional MHC class II system, is routed to MIICs, where it colocalizes with endogenous Ii molecules.

FRET studies indicate a physical interaction between CD70 and Ii

To examine whether Ii and CD70 physically interact in living cells, we performed FRET measurements. FRET is the transfer of energy from a donor fluorophore to a suitable acceptor fluorophore, which can be detected when the fluorophores are within an 80–100 Å range (Förster, 1948). Any significant FRET signal is therefore indicative of a physical interaction. Using EGFP as the donor fluorophore and mRFP as the acceptor fluorophore, we have previously demonstrated physical interactions between HLA-DR and HLA-DM in the internal vesicles of MIICs (Zwart et al., 2005). In the current study we fused EGFP to hIi-p33 as the donor and mRFP to mCD70 as the acceptor fluorophore and these chimeric proteins were expressed in HeLa cells. EGFP and mRFP were appended to the C-terminus of hIi-p33 and mCD70, respectively. Since both Ii and CD70 are type II transmembrane molecules, this implies that the fluorophores are localized in the lumen of the ER and MIICs and do not affect targeting signals located at the cytosolic site. Fusion with mRFP did not influence critical aspects of mCD70 trafficking, as outlined in Fig. 2. Moreover, the hIi–EGFP chimera physically interacted with human MHC class II and directed it to late endosomes and/or lysosomes, indicating that the EGFP fusion permitted normal MHC class II chaperone function of hIi-p33 (supplementary material Fig. S4A,B).

FRET experiments have to be extensively controlled (Zwart et al., 2005). To correct for leak-through of donor signal into the FRET channel and direct excitation of the acceptor fluorophore, the mCD70–mRFP- and hIi–EGFP-expressing HeLa cells were cocultured with control cells expressing histone 2B (H2B)–EGFP or H2B–mRFP as internal controls (Fig. 3A, I, II). FRET between hIi–EGFP and mCD70–mRFP was detected by CLSM as the sensitized emission of mRFP following energy transfer from EGFP (van Rheenen et al., 2004) (Fig. 3A, III). The sensitized emission images were corrected for spectral leak-through of EGFP into the mRFP channel and for indirect excitation of mRFP by the 488 nm laser used for exciting EGFP, using the H2B-fluorophore proteins, defining the remaining signal in the same sample as genuine FRET (Fig. 3A, IV). FRET was related to the total fluorescence emitted by the donor fluorophore to yield the donor FRET efficiency (E_D; Fig. 3A, V). E_D is the most relevant factor, as it is independent of donor fluorophore concentration. Fig. 3A, VI shows the distribution of E_D values of the pixels in panel V. Mean E_D between CD70 and Ii was 2%, well above the minimum detection limit (Zwart et al., 2005). We excluded an effect of pH on FRET by exposing cells to the lysosomotropic compound chloroquine for 2 minutes before imaging (Zwart et al., 2005). E_D was unaffected (Fig. 3B), excluding

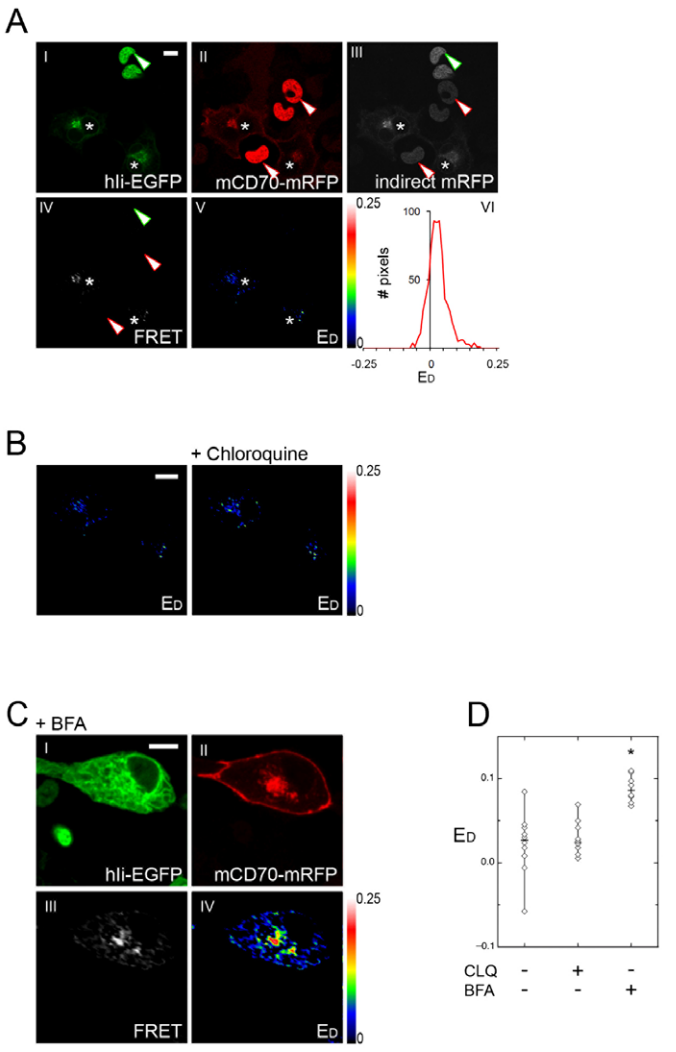

Fig. 3. FRET analysis to determine the physical interaction between CD70 and Ii. (**A**) HeLa cells were transfected to coexpress hIi–EGFP and mCD70–mRFP (asterisks). Control cells expressing either H2B–EGFP or H2B–mRFP were mixed into the same culture (arrowheads). All images are of the same sample: panel I, hIi–EGFP and H2B–EGFP in the green channel; II, mCD70–mRFP and H2B–mRFP in the red channel; III, the sensitized emission of mRFP following its activation by EGFP; IV, the corrected FRET signal between Ii–EGFP and mCD70–mRFP; V, the calculated donor FRET efficiency (E_D); and VI, the E_D value of each pixel shown as a histogram. The false color look-up table in V represents E_D values from 0 to 0.25, equaling 0–25% FRET efficiency. (**B**) Enlarged view of the mCD70-expressing cells depicted in A, V. E_D is shown before and after treatment of the sample for 2 minutes with chloroquine. (**C**) HeLa cells coexpressing hIi–EGFP and mCD70–mRFP were treated with BFA and incubated at 20°C. All signals are from the same sample. (**D**) E_D values from many samples in different experiments under conditions as in B,C, in which each data point represents one cell. BFA, brefeldin A; CLQ, chloroquine. Significant differences were determined with a two-tailed Student's *t*-test (**P*<0.05).

any direct effect of acidic pH in MIICs on fluorophore emission or FRET.

Ii binds MHC class II in the ER and escorts it through the Golgi complex to MIICs (Cresswell, 1994). We considered that Ii might similarly bind CD70 in the ER. To synchronize transport of such putative complexes, we treated cells with brefeldin A (BFA) to accumulate newly synthesized proteins in the ER (Klausner et al., 1992). Subsequently, BFA was removed and cells were cultured at 20°C. This allows protein egress from ER to the Golgi, but slows down further transport to post-Golgi locations (de Graaf et al., 2004). Under these conditions, E_D between Ii–EGFP and CD70–mRFP in the Golgi area was 8% (Fig. 3C,D). Taken together, these FRET measurements suggest that Ii physically interacts with CD70, which was particularly apparent in the Golgi area after synchronized transport from the ER.

CD70 and Ii form a complex in the ER without MHC class II

Next, we studied whether CD70 and Ii formed a complex by biochemical analysis. First, the intracellular transport of endogenous Ii, MHC class II and their potential complex formation with mCD70 were studied in Mel JuSo cells stably expressing unmodified mCD70 (Fig. 2B,C). These cells were left untreated or were stimulated with IFNγ to enhance Ii expression. Parental Mel JuSo cells were used as a control. Cells were metabolically pulse labeled followed by different chase periods. CD70, MHC class II and Ii were sequentially immunoprecipitated from the same lysates, and half of the samples were treated with endoglycosidase H (Endo H) to visualize transport of these glycoproteins out of the ER.

As expected, CD70 was expressed in the Mel JuSo CD70 cell line, but not in parental Mel JuSo cells (Fig. 4A, band 1). CD70 remained Endo H sensitive throughout the chase, consistent with the fact that mature CD70 at the cell surface still contains high mannose *N*-linked glycans (results not shown). Molecular species in the molecular mass range of 40–45 kDa were SDS-stable dimers of CD70 (results not shown) and an undefined Endo-H-sensitive glycoprotein (asterisk). In cells treated with IFNγ, an additional band was present in the CD70 isolate (band 2) that ran at the same position as a prominent molecular species present in the Ii isolate, and likewise was Endo H sensitive (Fig. 4B, band 2). Bands 2, 3 and 4 in the Ii isolate were Ii species, as determined by re-immunoprecipitation (supplementary material Fig. S5), in accordance with the literature (e.g. Machamer and Cresswell, 1982). Ii (band 2) was maturing during the chase, as indicated by the shift in molecular mass (band 3) and the appearance of Endo-H-resistant species (in supplementary material, compare Fig. S5B with E). In time, the Ii signal diminished, consistent with Ii degradation upon arrival at the MIIC (Neefjes and Ploegh, 1992; Cresswell, 1994). From early time points onward, MHC class II was isolated with Ii, as was demonstrated by re-immunoprecipitation of Ii (supplementary material Fig. S5). CD70 comigrated with the MHC class II β chain, before and after Endo H digestion, which hampered identification of CD70 in the Ii and/or MHC class II isolates. This experiment suggested complex formation between CD70 and Ii and indicated that CD70 did not affect assembly and intracellular transport of the MHC class II–Ii complex.

To examine the interaction of Ii with CD70 without involvement of MHC class II and with potentially stronger CD70 and Ii signals, we transiently coexpressed CD70 and Ii in HeLa cells. In this case, we analyzed murine CD70 in the presence or absence of the murine p31 (mIi–p31) or p41 Ii (mIi–p41) isoforms. Pulse–chase labeling was performed as for Mel JuSo cells and CD70 and Ii were immunoprecipitated in parallel from split cell lysates. From HeLa cells expressing mCD70 alone, mCD70 was readily isolated (band 1) and its SDS-resistant dimer was also visible (Fig. 5). From the HeLa cells that coexpressed either mIi–p31 or mIi–p41, mCD70 was isolated together with small amounts of these Ii species, as

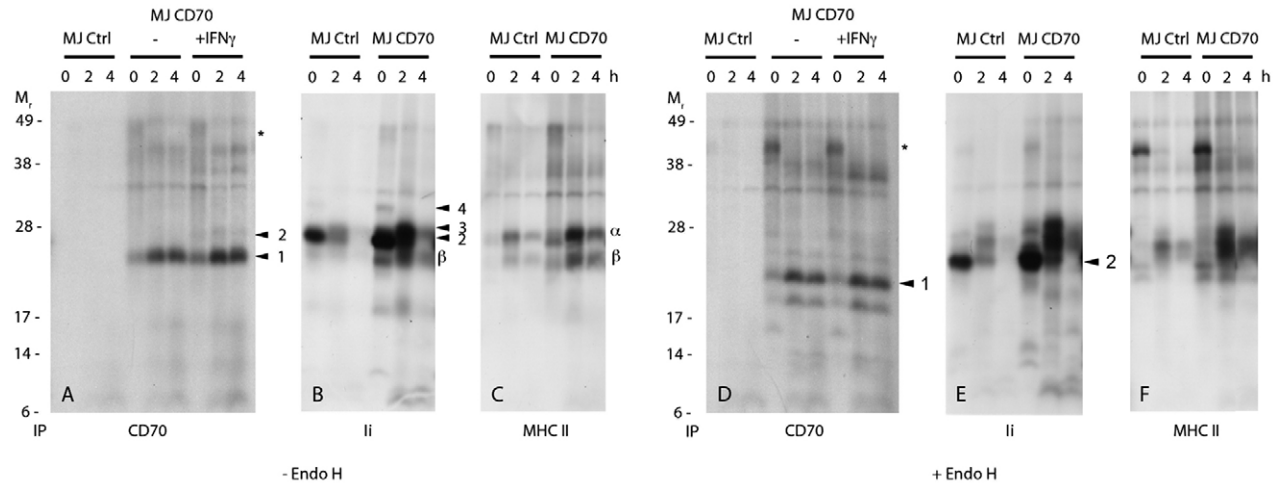

Fig. 4. Biosynthesis and maturation of CD70, Ii and MHC class II in Mel JuSo cells. Parental Mel JuSo cells (MJ Ctrl) and Mel JuSo cells stably expressing mCD70 (MJ CD70) were stimulated or not with IFNγ and subsequently pulse labeled with [^{35}S]methionine and [^{35}S]cysteine for 1 hour. Cells were harvested directly after the pulse (0 hours), or after an additional 2 hours or 4 hours chase period. Sequential specific immunoprecipitation (IP) with antibodies to mCD70, MHC class II and Ii was performed and samples were mock incubated or subjected to Endo-H treatment. Samples were resolved by SDS-PAGE under reducing conditions on home-cast large 10-15% gradient gels. Relative mol mass (M_r, $\times 10^{-3}$) is indicated by prestained NuPAGE mol mass markers. The position of CD70 (1) and Ii species (2,3,4) in the respective IPs are indicated, as well as MHC class II α and β chains. The asterisk indicates an undefined protein in the CD70 IP at *t*=0 of the chase. Ii species were defined in the Ii IP by reimmunoprecipitation, as shown in supplementary material Fig. S5.

identified by the parallel Ii immunoprecipitation (band 2, mIi–p31; band 3, mIi–p41). The association between mCD70 and mIi–p31 or mIi–p41 was most apparent at the 0 hours chase time point, remained detectable at the 1 and 2 hours chase time points and later disappeared. Accordingly, the Ii immunoprecipitates show that the Ii signal gradually diminished with time, in agreement with degradation of Ii upon arrival at the MIIC. Conversely, some mCD70 was present in the Ii isolates, as most clearly seen for mIi–p31. Since HeLa cells do not express endogenous MHC class II, these data indicate that mCD70 can form an MHC class II-independent complex with either the p31 or the p41 isoform of murine Ii in the ER, soon after biosynthesis.

Ii regulates transport of CD70 from the Golgi to the MIIC in primary DCs

Next, we extended our observations from model cell lines to primary DCs. To determine the impact of endogenous Ii on the subcellular localization of endogenous CD70 we compared bone marrow (BM)-derived DCs from wild-type (WT) mice and Ii-deficient (*Ii*$^{-/-}$) mice (Viville et al., 1993). To induce CD70 expression and to follow CD70 protein transport upon DC maturation, DCs were stimulated with TLR ligand lipopolysaccharide (LPS) for 5, 10 or 20 hours. Immunoblotting confirmed CD70 protein expression in these DC preparations (results not shown). To monitor localization of CD70, we used LAMP1 as a marker for the late endosomal and/or lysosomal MIICs (Vyas et al., 2007) and p115 as a marker for the Golgi (Nakamura et al., 1997). Staining for MHC class II in serial samples confirmed that the LAMP1-positive compartments were MIICs (results not shown; see also supplementary material Fig. S8). Pearson's correlation coefficients were calculated for WT and *Ii*$^{-/-}$ DCs for each time point, to quantify the correlations between CD70–LAMP1 and CD70–Golgi signals.

The transmission images in Fig. 6A,B illustrate the morphological changes that WT and *Ii*$^{-/-}$ DCs underwent upon maturation by 20 hours of LPS stimulation. Staining for Ii confirmed the WT (Fig. 6A) and *Ii*$^{-/-}$ (Fig. 6B) genotype of the DCs. Ii resided at the nuclear envelope and the associated ER network as well as in LAMP1-positive compartments (Fig. 6A and results not shown). As described previously for activated primary DCs (Villadangos et al., 2001), LAMP1-positive compartments were highly concentrated in an area of the cell that also contained the Golgi (Fig. 6A,B). In WT DCs that had been matured with LPS for 5 hours, CD70 was not specifically enriched in Golgi or LAMP1-positive vesicles, as determined by the average Pearson's correlation coefficients (*r*-values; Fig. 6D). Upon DC maturation

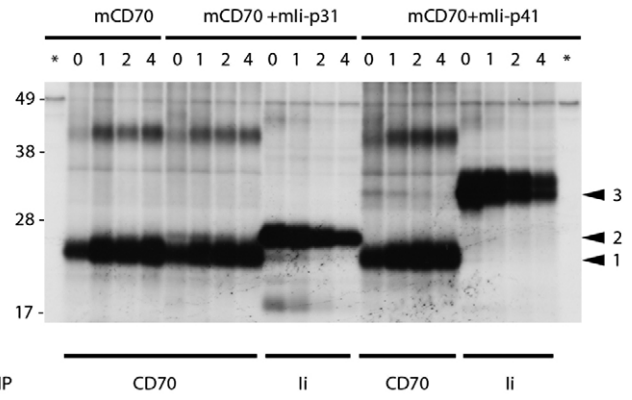

Fig. 5. Murine p31 and p41 Ii associate with mCD70 at an early time point after biosynthesis. HeLa cells were transfected to express mCD70 alone, or together with either the p31 or the p41 isoform of murine Ii. Cells were pulse labeled for 1 hour with a mixture of [^{35}S]methionine and [^{35}S]cysteine and harvested following chase periods of 0, 1, 2 or 4 hours. Lysates were prepared, divided, and mCD70 was immunoprecipitated with FR70 mAb from one half and mIi-p31 or mIi-p41 were immunoprecipitated with S22 serum from the other half of the same lysates (parallel IP). Samples were resolved by SDS-PAGE as outlined for Fig. 4. The asterisks indicate isolates with an irrelevant antibody. The arrowheads indicate the positions of mCD70 (1), mIi-p31 (2) and mIi-p41 (3). The experiment was repeated with similar results.

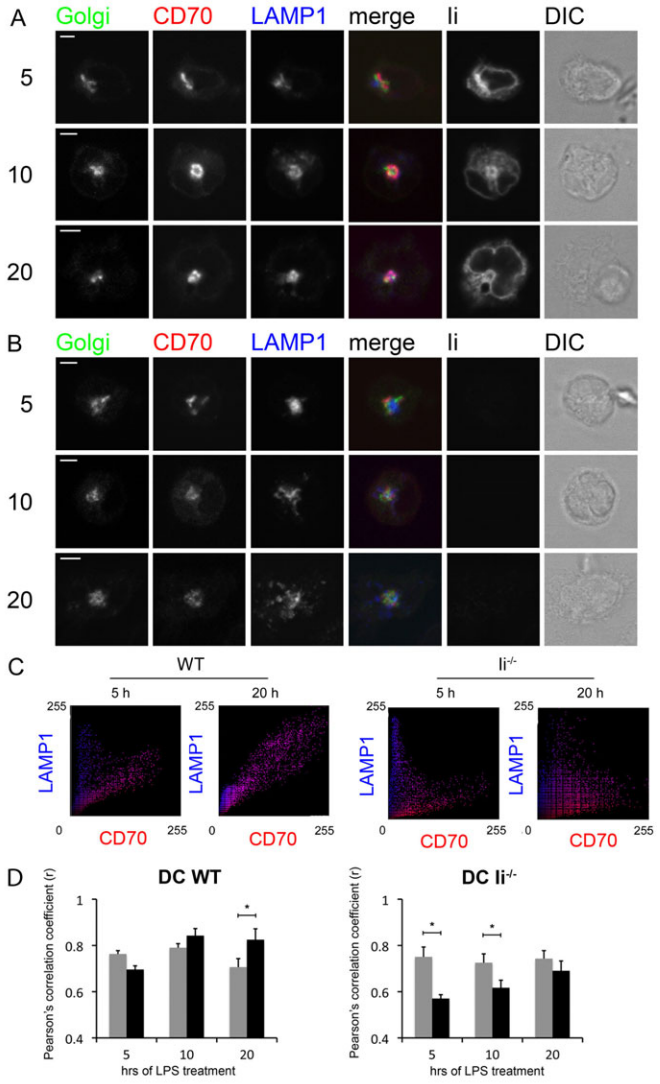

Fig. 6. Temporal analysis of Ii-guided CD70 transport in primary bone marrow-derived DCs. BM-derived DCs from WT (**A**) or $Ii^{-/-}$ (**B**) mice were matured with LPS for 5, 10 or 20 hours. Subsequently, cells were fixed, permeabilized and stained with rat anti-mCD70 (FR70) and goat anti-rat Ig–Alexa Fluor 568, in combination with rabbit anti-Ii (S22) and goat anti-rabbit Ig–Alexa Fluor 647. After overnight blocking with 0.25% BSA in PBS, samples were stained with rat anti-LAMP1 and goat anti-rat Ig–Alexa Fluor 488 in combination with mouse anti-mouse Golgi marker (p115) and goat anti-mouse Ig–Alexa Fluor 405. (A,B) CLSM analysis. Colocalization of the Golgi (green), CD70 (red) and LAMP1 (blue) signals is shown in the merged image. Images are representative of two independent experiments (n>30). DIC, differential interference contrast. Scale bars: 5 µm. (**C**) Scatter plot analysis of CLSM images from A and B. CD70 versus LAMP1 signal distribution in WT or $Ii^{-/-}$ DCs at 5 or 20 hours after LPS stimulation. (**D**) Pearson's correlation coefficients (r) from at least eight independent images per condition, indicating the correlations between CD70–Golgi signals (gray) and CD70–LAMP1 signals (black). Significant differences were determined with a two-tailed Student's t-test (*P≤0.05).

for 10–20 hours, however, CD70 progressively relocated to LAMP1-positive compartments (Fig. 6A, purple color in the merged image), which was substantiated by scatter plot analyses (Fig. 6C; supplementary material Fig. S6) and quantified as a significant difference in the r-values for CD70–LAMP1 versus CD70–Golgi signals at the 20 hours time point (Fig. 6D). Importantly, the progressive relocation of CD70 towards LAMP1-positive compartments upon DC maturation was impaired in $Ii^{-/-}$ DCs. This was apparent from the primary CLSM data (Fig. 6B) and associated scatter plot analyses (Fig. 6C; supplementary material Fig. S6), as well as from the quantification of colocalization that, in contrast to the WT situation, revealed no significant difference between the r-values for CD70–Golgi and CD70–LAMP1 at the 20 hours time point (Fig. 6D). Rather, the quantitative analysis revealed a significant enrichment of CD70 in the Golgi of $Ii^{-/-}$ DCs at the 5 and 10 hours time points. Since this was not observed in WT DCs, these data indicate that CD70 transport was arrested in the Golgi due to Ii deficiency. We conclude that in maturing DCs, CD70 does not need Ii to exit the ER, but requires Ii to travel from the Golgi to the late endosomal and/or lysosomal MIICs. At 20 hours, CD70 did not colocalize with EEA1, a marker for early endosomes (supplementary material Fig. S7), in accordance with our previous findings in Mel JuSo cells (Keller et al., 2007).

To extend these findings, we studied spleen-derived DCs and examined the dependence of CD70 transport on MHC class II, making use of DCs from MHC class II deficient ($MHC\text{-}II^{-/-}$) mice (Cosgrove et al., 1991). Localization of CD70 was compared in LPS-activated WT, $Ii^{-/-}$ and $MHC\text{-}II^{-/-}$ DCs. Staining for MHC class II confirmed the genotype of the $MHC\text{-}II^{-/-}$ DCs (supplementary material Fig. S8A). In WT DCs, MHC class II was enriched in LAMP1-positive compartments (MIICs), as expected, as was evident from the images, scatter plots and quantifications (supplementary material Fig. S8A–C). In $Ii^{-/-}$ DCs, MHC class II was not enriched in LAMP1-positive compartments and primarily located at the nuclear envelope and ER network (supplementary material Fig. S8A–C), in accordance with the described role of Ii in ER exit of MHC class II (Marks et al., 1990). In $MHC\text{-}II^{-/-}$ DCs, Ii was expressed, but also primarily localized to the nuclear envelope and ER network (Fig. 7A).

As in BM-derived DCs, CD70 showed a much more pronounced localization to LAMP1-positive compartments in WT DCs than in $Ii^{-/-}$ DCs, as documented by CLSM (Fig. 7A), associated scatter plot analyses (Fig. 7B) and quantification of colocalization (Fig. 7C). In $Ii^{-/-}$ DCs, CD70 signal instead was enriched in the Golgi, as can be appreciated from the scatter plot analyses (Fig. 7B) and was found to be significant by quantification of the colocalization (Fig. 7C). In $MHC\text{-}II^{-/-}$ DCs, CD70 had a similar distribution as in WT DCs: CD70 signal was significantly enriched in LAMP1-positive structures (Fig. 7A–C). We conclude that Ii is required to transport CD70 from the Golgi to MIICs and does so in an MHC class II-independent fashion.

Discussion

We have shown previously that in activated conventional DCs, newly synthesized CD70 is directed to MIICs. This allows for the coordinated vesicular transport of both CD70 and MHC class II molecules to the immunological synapse that is formed when a DC contacts an antigen-specific $CD4^+$ T cell. In this way, CD70–CD27 co-stimulation is temporally and spatially coordinated with MHC class II antigen presentation and consequent TCR triggering (Keller et al., 2007). Here, we reveal the molecular basis of this process: CD70 is guided to MIICs by Ii, the chaperone protein that also escorts MHC class II molecules to the same late endosomal and/or lysosomal compartments. We demonstrate that CD70 and Ii form

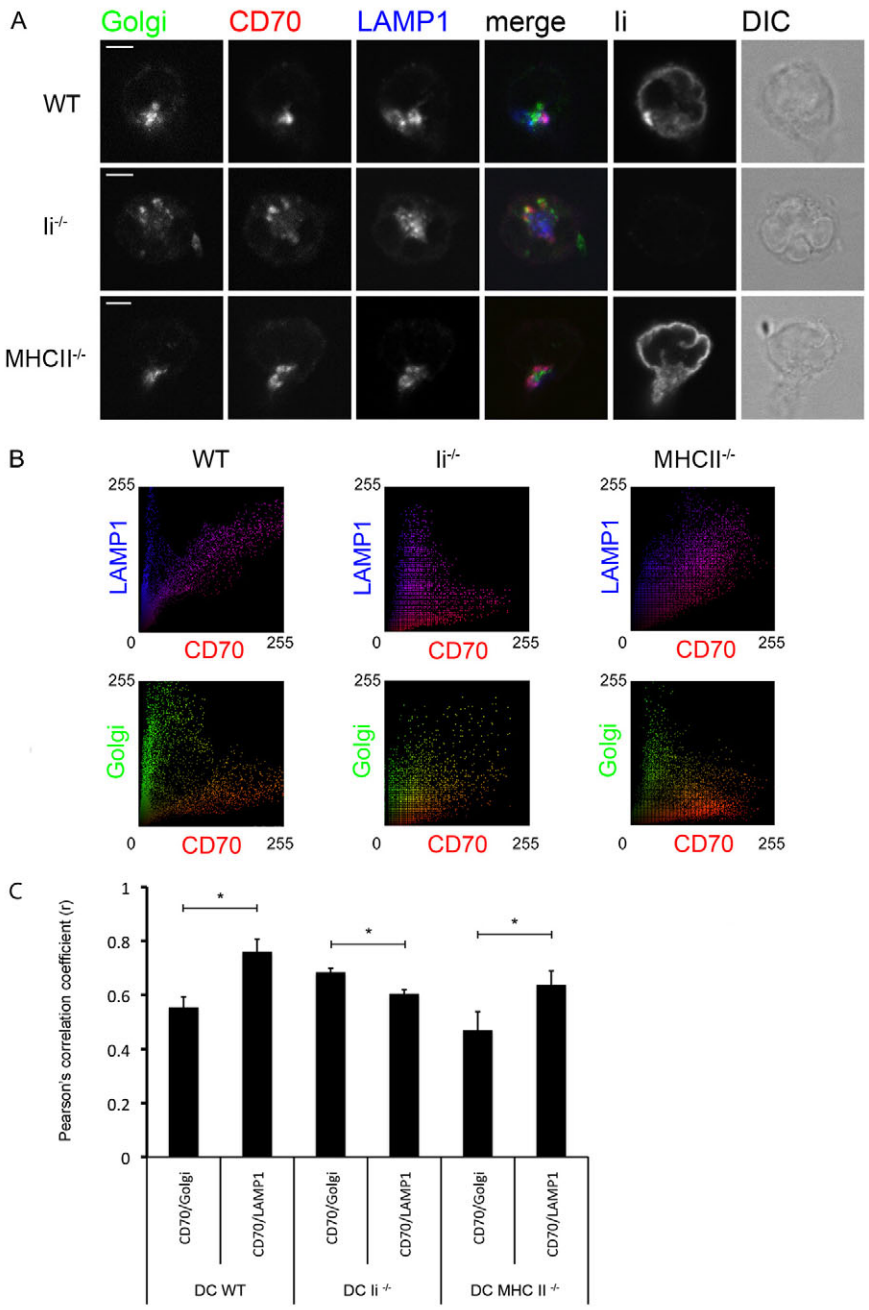

Fig. 7. Influence of Ii or MHC class II on CD70 transport in splenic DCs. Splenic DCs from WT, $Ii^{-/-}$ or *MHC-II*$^{-/-}$ mice were matured with LPS for 7 hours and stained using the same procedures as described in Fig. 5. (**A**) CLSM analysis. The merged image shows colocalization between the Golgi apparatus (green), CD70 (red) and LAMP1 (blue). Images are representative of two independent experiments (n>25). DIC, differential interference contrast image. Scale bars: 5 µm. (**B**) Scatter plot analysis of CLSM images from A. CD70 versus LAMP1 or Golgi signal distribution in WT, $Ii^{-/-}$ and *MHC–II*$^{-/-}$ DCs. (**C**) Pearson's correlation coefficients (r) from six independent images per condition, indicating the correlations between CD70–Golgi and CD70–LAMP1 signals for WT, $Ii^{-/-}$ or *MHC–II*$^{-/-}$ DCs. Significant differences were determined with a two-tailed Student's t-test (*P≤0.05).

a physical complex that is MHC class II-independent and that Ii is required to direct CD70 from the Golgi to late endosomal MIICs.

The chaperone function of Ii for MHC class II is documented in detail (Cresswell, 1994; Jasanoff et al., 1998). In the ER, Ii forms a homotrimer and interacts with three MHC class II αβ heterodimers to form a nonameric complex. Di-leucine-based motifs in the cytoplasmic tail of Ii subsequently direct the complex to MIICs (Cresswell, 1994; Michelsen et al., 2005). This may occur directly from the trans-Golgi network, but can also involve routing via the plasma membrane (Bénaroch et al., 1995; McCormick et al., 2005; Dugast et al., 2005). Ii also performs such a chaperone function for CD1d (Kang and Cresswell, 2002; Jayawardena-Wolf et al., 2001) and for the neonatal Fcγ receptor (Ye et al., 2008), both of which are closely related to MHC molecules. A chaperone function of Ii for CD70 is unusual in this context, because the structure of TNF family members is distinct from that of MHC-like molecules (Banner et al., 1993).

We show that Ii expression redirects CD70 transport in HeLa cells from the cell surface towards lysosomes. However, genetic evidence does not suffice to say that Ii acts as an actual chaperone of CD70, since Ii (over)expression may alter endosome structure and dynamics (e.g. Romagnoli et al., 1993). Therefore, we aimed to establish whether Ii physically interacts with CD70, as is expected for a chaperone. Our biochemical data indicate that CD70 and Ii form a complex that is independent of MHC class II. Although the biochemistry and FRET data cannot provide unambiguous evidence for a direct rather than indirect interaction between CD70 and Ii, on the basis of their overall structural

homology, it is plausible that CD70 and Ii interact directly: both are type II transmembrane glycoproteins, with a cytoplasmic tail of 22–28 amino acids and an extracellular (luminal) domain of about 150 amino acids (Goodwin et al., 1993; Tesselaar et al., 1997). Moreover, Ii is a trimer and CD70, like other TNF family members, is most probably a trimer as well. However, the exact mechanism of CD70–Ii interactions must be distinct from MHC class II–Ii interactions, given the structural differences between CD70 and MHC class II. In the case of the MHC class II αβ heterodimer, the peptide binding groove binds the CLIP region of Ii (Jasanoff et al., 1998). CD70 does not have an analogous CLIP-binding region, as predicted from the crystal structure of TNF (Banner et al., 1993) and related proteins.

In both human and mouse, Ii exists in different isoforms, which are generated by alternative splicing, as well as by alternative translation initiation (Strubin et al., 1986; O'Sullivan et al., 1987). The p31 and p41 mouse isoforms used in this study arise from alternative splicing of exon 6b that encodes a cysteine-rich luminal domain (Koch et al., 1987a) (supplementary material Table S1). The human Ii gene similarly encodes p35 and p43 isoforms that differ in exon 6b. The human p33 isoform we have used here is endogenously generated from p35 mRNA (isoform 2b, NP_004346.1) via an alternative translation start site (see supplementary material Table S1). This shortens the cytoplasmic tail and deletes the arginine-based motif that contributes to its retention in the ER (Michelsen et al., 2005). However, hIi-p33 had a predominant ER localization when expressed alone in HeLa cells. CD70 coexpression released part of the Ii pool from the ER (data not shown) and supported transport to CD63-positive compartments (Fig. 1).

Co-immunoprecipitation experiments showed that mCD70 associates with both p31 and p41 isoforms of murine Ii in HeLa cells. The exon 6b-encoded luminal domain that is uniquely present in mIi-p41 is apparently not crucial for CD70–Ii interaction, but the exact sites of interaction still have to be determined. Since DCs express very low levels of CD70, it is difficult to study the endogenous interactions between CD70 and Ii. Even upon exogenous expression of CD70, we could visualize CD70–Ii complexes only in biosynthetic labeling experiments, but not by immunoblotting (results not shown). This is explained by the fact that immunoblotting detects the total intracellular pool of protein and does not focus on the newly synthesized one, which is particularly important in this case, because Ii is degraded upon arrival at the MIICs. In the same immunoblotting experiments, we observed Ii in association with MHC class II. Therefore, complexes between Ii and CD70 are more difficult to isolate, possibly because detergent lysis results to some extent in their dissociation.

We have demonstrated that CD70 forms a complex with mIi-p31 or mIi-p41 early after biosynthesis upon coexpression in HeLa cells. These complexes were endoglycosidase H sensitive (results not shown) and therefore they were located in the ER. In Mel JuSo cells, the increase in FRET signal between Ii and CD70 in the Golgi after BFA pretreatment and release supports the scenario that CD70 and Ii form a complex in the ER that moves through the Golgi. The FRET signal between CD70–mRFP and Ii–GFP was lower in MIICs than in the Golgi after BFA treatment. This suggests that interactions between CD70 and Ii are lost upon arrival at MIICs, probably because of degradation of Ii, analogous with the situation for Ii–MHC class II complexes (Cresswell, 1994). The biochemical pulse–chase experiments also suggest that Ii is lost from CD70 upon its degradation in MIICs.

Our studies with WT and $Ii^{-/-}$ DCs showed that CD70 does not require Ii to exit the ER and travel through the Golgi, but relies on Ii for efficient transport from the Golgi to MIICs. In WT DCs (this study) and in Mel JuSo cells (Keller et al., 2007) many CD70 molecules resided in the Golgi at steady state conditions, in line with regulation of its intracellular transport at this site. In WT DCs, we found no CD70 in early endosomes, suggesting that CD70–Ii complexes predominantly travel directly from the Golgi to MIICs, which is also the major route for MHC class II (Bénaroch et al., 1995). This, however, does not exclude alternatives such as rapid transfer over the plasma membrane by a minor fraction of molecules. We found that in $Ii^{-/-}$ DCs, CD70 eventually did appear in LAMP1-positive structures, but this trafficking was greatly delayed compared with the WT situation, and still incomplete at 20 hours after DC stimulation. This suggests that an alternative, yet significantly less efficient, Ii-independent route exists for CD70 to move to LAMP1-positive structures from the Golgi, possibly via the cell surface. We did not find an enhanced cell surface expression of CD70 in $Ii^{-/-}$ DCs as compared with WT DCs (results not shown). Since in HeLa cells, CD70 traveled to the cell surface in absence of Ii, this alludes to additional Ii-independent control mechanisms of CD70 transport in professional antigen-presenting cells that are currently undefined.

MIICs are multivesicular bodies, specialized endosomal compartments that generally are composed of a limiting membrane surrounding many internal vesicles (e.g. Peters et al., 1991). These internal vesicles are formed by budding off from the limiting membrane. The immuno-EM demonstrated CD70 and Ii primarily on the internal vesicles of MIICs in Mel JuSo cells. The Ii that we detected may be intact, or luminally degraded, since the antibody used reacts with a cytoplasmic epitope. Previously, we showed colocalization of CD70 and MHC class II at this location (Keller et al., 2007). Sorting of MHC class II to internal vesicles of MIICs is guided by its ubiquitylation (van Niel et al., 2006) and it will be of interest to determine how this occurs for CD70. Multivesicular bodies can mature into lysosomes, resulting in the degradation of their protein cargo. However, the content of MIICs can also be transported back to the plasma membrane, via mechanisms that are only partially defined. For example, it has been observed that in DCs, multivesicular MIICs can dramatically alter their morphology upon activation, changing from vacuolar to long tubular organelles. In this process, MHC class II relocates from the internal vesicles to the limiting membrane of the tubules. Polarization of these tubules towards antigen-specific T cells required a TLR and a TCR signal, and vesicles derived from the tubules were suggested to deliver MHC class II to the plasma membrane (Kleijmeer et al., 2001; Boes et al., 2002; Boes et al., 2003; Chow et al., 2002). Like MHC class II, CD70 may relocate from internal vesicles to the limiting membrane of the MIICs during their morphological transformation and thus be rescued from degradation. However, also multivesicular MIICs are expected to travel towards the synapse because of the orientation of the microtubular cytoskeleton, before fusing with the plasma membrane (Wubbolts et al., 1996). This scenario is more reminiscent of what we have observed thus far studying DC–$CD4^+$ T cell conjugates (Keller et al., 2007). Upon exocytosis of such MIICs, the internal vesicles containing CD70 and MHC class II may fuse back to the limiting membrane of MIICs and then fuse with the plasma membrane of the DC. The molecular details of this process are as yet obscure.

In conclusion, we define a novel target for the chaperone Ii that is not an MHC family member, but the TNF family member CD70.

Ii is essential for transport of CD70 to MIIC structures, which brings the cell surface deposition of CD70 under the same cell biological control as MHC class II molecules. As a consequence, antigen-loaded MHC class II molecules will be delivered along with CD70 at the immune synapse that is formed between an antigen-specific $CD4^+$ T cell and a DC, thus coordinating TCR stimulation with CD27 co-stimulation.

Materials and Methods

Mice

Wild-type, *Ii*$^{-/-}$ (Viville et al., 1993) and *MHC-II*$^{-/-}$ (Cosgrove et al., 1991) mice in a C57BL/6 background were used at 6- to 12-weeks of age. Experiments were performed in agreement with national and institutional guidelines.

Antibodies

Monoclonal antibodies used were: mouse anti-human CD63, MEM-259; rat anti-mouse CD70, FR70 (Oshima et al., 1998); mouse anti-human CD70, 2F2 (Hintzen et al., 1994); mouse anti-human Ii, Bu45; mouse anti-human MHC class II DRα, 1B5 (Neefjes et al., 1990); rat anti-mouse LAMP1, 1D4B; mouse anti-mouse p115 (BD Biosciences, catalog number 612260). Polyclonal rabbit sera used were: anti-human Ii, ICN1 (Morton et al., 1995); anti-mouse Ii, S22 (Koch et al., 1987b); anti-mouse MHC class II (I-A^bβ) JV2 (Bryant et al., 1999), anti-EEA1 (Abcam, ab2900). For CLSM, MEM-259 was used as FITC conjugate, other antibodies were used as purified immunoglobulin or serum and detected by secondary antibodies, conjugated to fluorochromes (Molecular Probes), as indicated.

Cell isolation and culture

The human melanoma cell line Mel JuSo, the human cervix carcinoma cell line HeLa and their stably transduced or transfected derivatives were grown in IMDM (Gibco-BRL) supplemented with 8% FCS, penicillin and streptomycin. DCs were generated from bone marrow as described previously (Naik et al., 2005). Briefly, bone marrow cells were isolated and cultured for 8–10 days in the presence of recombinant Flt3 ligand (generated in-house). For generation of splenic DC, mice were injected subcutaneously with 4×10^6 Flt3 ligand-expressing B16 tumor cells, spleens were isolated 12 days later and digested for 20 minutes at room temperature with 1 mg/ml collagenase D (Roche) and 0.1 mg/ml DNAse (Roche). Cells were passed through a 70 μm cell filter (BD Biosciences) and DCs were isolated using CD11c MACS beads (Miltenyi Biotec). DCs were matured by incubation with 1 μg/ml LPS of *Escherichia coli* serotype 055:B5 (Sigma-Aldrich) in RPMI supplemented with 10% FCS, penicillin, streptomycin and 50 μM 2-mercaptoethanol. DC viability was checked by light microscopy and Trypan Blue exclusion and was over 90% in all experiments.

Constructs and gene transfer

The Mel JuSo cell line stably expressing murine (m)CD70 was generated by retroviral transduction as described previously (Keller et al., 2007). Transient transfection of Mel JuSo or HeLa cells with cDNA encoding mCD70 (Tesselaar et al., 1997), human CD70 (Goodwin et al., 1993), human Ii-p33 (all in pcDNA3 expression vector), or mouse Ii-p31 or Ii-p41 was performed using Fugene 6 Transfection Reagent (Roche). For FRET experiments, constructs were used encoding mCD70–mRFP and human (h)Ii-p33–EGFP. m*Cd70* cDNA was cloned into pmRFP-N1 and Ii into pEGFP-N1 (Clontech). pmRFP-N1 was derived from pEGFP-N1 by replacing the EGFP-coding sequence with the mRFP coding sequence using *Bam*HI and *Not*I sites. pcDNA3 expression constructs encoding histone 2B–GFP (H2B–GFP), or –mRFP (H2B–mRFP) were used as controls for FRET experiments (van Rheenen et al., 2004). The constructs pFM332.1=pHbAPr1-neo with mouse *p41* cDNA and pFM338.1=pHbAPr1-neo with mouse *p31* cDNA were kindly provided by Frank Momburg (German Cancer Research Institute, Heidelberg, Germany). The pHbAPr1-neo plasmid contains the human β actin promoter and was used directly for transfection into HeLa cells. All constructs were verified by nucleotide sequencing.

Confocal laser scanning microscopy

HeLa cells transfected with *Ii* and/or *Cd70* cDNA were allowed to attach to glass coverslips for 24 hours. DCs were allowed to attach for 1 hour to coverslips coated with poly-L-lysine (Sigma Aldrich). Cells were washed in PBS containing 1 mM $MgCl_2$ and 1 mM $CaCl_2$, fixed for 10 minutes with 3.7% paraformaldehyde in PBS, permeabilized for 3 minutes with 0.1% Triton X-100 in PBS and blocked for 30 minutes using 1% BSA in PBS. Incubations were performed with antibodies diluted in blocking buffer for 45 minutes, after which coverslips were washed and incubated for 30 minutes with the appropriate secondary antibodies diluted in blocking buffer. Coverslips were washed, mounted in Vectashield (Vector Laboratories) and viewed under a Leica TCS NT CLSM microscope (Leica Microsystems). Images with two fluorochromes were taken by simultaneous scanning, and images with three fluorochromes were taken by sequential scanning. Antibody cross-reactivity was excluded since non-specific combinations of primary and secondary antibodies did not show any staining (data not shown). Pixel distribution scatter plots for colocalization analysis (in which the signal intensity per pixel in every channel was related to the other channels and plotted in a 2D graph) and Pearson's correlation coefficients were generated with the Intensity Correlation Analysis function of the WCIF plugin of ImageJ (www.uhnresearch.ca/wcif).

Immuno-electron microscopy

Mel JuSo cells stably expressing mCD70 were fixed for 2 hours in a mixture of 2% paraformaldehyde and 0.2% glutaraldehyde in 60 mM PIPES, 25 mM HEPES, 2 mM $MgCl_2$, 10 mM EGTA, pH 6.9 and processed for ultrathin cryosectioning as described previously (Calafat et al., 1997). For immunolabeling, the sections were incubated for 10 minutes with 0.15 M glycine in PBS and for 10 minutes with 1% BSA in PBS. Thereafter they were incubated with anti-Ii rabbit polyclonal immunoglobulin ICN1 and 10 nm protein-A-conjugated colloidal gold (EM lab, University of Utrecht) in 1% BSA in PBS. Next, sections were fixed in 1% glutaraldehyde and blocked with glycine and BSA in PBS, incubated with anti-mCD70 mAb FR70 for 1 hour, followed by rabbit anti-rat immunoglobulin adsorbed against mouse immunoglobulin, followed by a 15-nm protein-A-conjugated gold probe. Next, the cryosections were embedded in uranylacetate and methylcellulose and examined with a Philips CM 10 electron microscope (FEI Eindhoven, The Netherlands).

FRET imaging

HeLa cells were cultured on coverslips for 48 hours. At 24 hours prior to imaging, cells were transfected to express Ii–EGFP and CD70–mRFP. Mel JuSo cells stably transfected to express H2B–GFP or H2B–mRFP were added to the culture for leak-through corrections and internal controls as described previously (Zwart et al., 2005). For imaging, coverslips were placed in 2 ml bicarbonate-buffered saline (140 mM NaCl, 5 mM KCl_2, 2 mM $MgCl_2$, 1 mM $CaCl_2$, 23 mM $NaHCO_3$, 10 mM D-glucose, 10 mM HEPES pH 7.3) and analyzed in a tissue culture chamber at 37°C, 5% CO_2. FRET between EGFP and mRFP was determined by calculating the sensitized emission (the mRFP emission upon EGFP excitation), using separately acquired donor and acceptor images as described previously (van Rheenen et al., 2004). In short, images were acquired on a DM-Ire2 inverted microscope fitted with a TCS-SP2 scan head (Leica Microsystems). Three images were collected: EGFP excited at 488 nm and detected at 495–550 nm; indirect mRFP excited at 488 nm and detected at 580–650 nm and direct mRFP excited at 568 nm and detected at 580–650 nm. Because of considerable overlap of the EGFP and mRFP spectra, mRFP emission was corrected for leak-through of EGFP emission and for direct excitation of mRFP during EGFP excitation. FRET was calculated from these data (Forster, 1948), with shade correction and smoothening of images. Sensitized emission (FRET) was calculated using correction factors obtained from cells expressing either GFP or mRFP alone, which were included for every image. The apparent donor FRET efficiency (E_D) was calculated by relating the FRET signal to the total emission signal of the donor fluorophore, after which the E_D image was overlaid with a false color look up table. By this approach, differences in FRET efficiency can be measured with an accuracy of 0.5% (Zwart et al., 2005). For graphic representation, the E_D was calculated for each pixel from the raw data files of the represented cell and was exported to Microsoft Excel. In this program, the number of pixels was related to the corresponding E_D and plotted as a histogram. Brefeldin A (GolgiPlug, BD Biosciences) was added to the cells for 6 hours, washed off, and cells were subsequently incubated for 1 hour at 20°C. Where indicated, chloroquine (200 μM) was added to the cells for 2 minutes prior to imaging, to neutralize late endosomes and/or lysosomes (Zwart et al., 2005 and results not shown).

Metabolic labeling and immunoprecipitation

For metabolic labeling, parental Mel JuSo cells and Mel JuSo cells stably expressing mCD70 were plated at 0.75×10^6 cells per 10 cm dish. Mel JuSo mCD70 cells were cultured in the presence or absence of 300 ng/ml IFNγ (Reprotech). Three dishes were used for each cell population. After overnight culture, cells were starved in methionine- and cysteine-free DMEM for 2 hours, and pulse labeled with [^{35}S]methionine and [^{35}S]cysteine mixture (9 MBq per dish; NEN, Boston, MA) for 1 hour in the same medium. For the chase, cells were cultured for an additional 2 or 4 hours in complete DMEM medium, supplemented with unlabeled methionine and cysteine (2.5 mM). At the harvesting time points, medium was removed, cells were washed with PBS and lysed in immunoprecipitation (IP) buffer (10 mM Tris–HCl, pH 7.8, 150 mM NaCl, 1 mM PMSF and Complete EDTA-free Protease Inhibitors (Roche Molecular Biochemicals) with 1% Brij96 detergent. Lysates were cleared by centrifugation for 15 minutes at 13,000 ***g*** and precleared extensively with protein-G–Sepharose beads (Pharmacia) and irrelevant antibody. Next, specific IP was performed with anti-mCD70 mAb FR70, followed by anti-MHC class II mAb 1B5 and anti-Ii mAb VIC-Y1, all in combination with Protein G beads. Following each specific IP, mAb was cleared from the lysates by incubation with Protein-G beads. HeLa cells were plated at 0.5×10^6 cells per 10 cm dish and transfected the next day with m*Cd70* cDNA in the presence or absence of m*Ii-p31* or m*Ii-p41* cDNA. Four dishes were used for each cell population. Cells were metabolically pulse–chase labeled and lysed as outlined above. Lysates were precleared and split in equal parts. Specific IP was performed from each part with either anti-mCD70 mAb FR70 or anti-Ii serum S22 in combination with Protein-G beads. Immunoprecipitates were taken up in reducing SDS sample buffer and samples were heated for 10 minutes at

95°C prior to electrophoresis. For Endo-H treatment, immunoprecipitates were taken up in 50 mM sodium citrate, pH 5.5, with 0.2% SDS and heated for 5 minutes at 55°C. Next, they were mock incubated or treated with 2 mU Endoglycosidase H (Roche) overnight at 37°C. Concentrated reducing SDS sample buffer was added and samples were heated for 10 minutes at 95°C. SDS-PAGE was performed on home-cast large 10–15% gradient gels. The same prestained NuPAGE molecular mass markers (See Blue Plus2, Invitrogen) were used for all gels. Gels were fixed, washed in water, incubated in 1 M sodium salicylate pH 6 for 45 minutes, dried and subjected to autoradiography.

Reimmunoprecipitation

For reimmunoprecipitation from Ii IPs, protein-G–VICY1 bead isolates were taken up in IP buffer with 1% Nonidet P40 and 1% SDS and heated for 5 minutes at 68°C. Next, dithiothreitol was added to 2 mM and samples were incubated for 30 minutes at 45°C, followed by addition of iodoacetamide to 20 mM and incubation for a further 20 minutes at room temperature. Next, samples were diluted tenfold with IP buffer containing 1% Nonidet P40, 100 μg RNAse A was added as carrier protein, Protein G beads were removed by centrifugation and the supernatant was subjected first to non-specific IP with irrelevant mAb and then to specific IP with VICY1 anti-human Ii mAb.

We thank B. Dubois and D. Kaiserlian (University of Lyon, Lyon, France) for providing *Ii*$^{-/-}$ mice, N. Koch (Bonn University, Bonn, Germany) for the gift of anti-Ii antibodies, and F. Momburg (German Cancer Research Center, Heidelberg, Germany) for provision of the murine Ii constructs. We thank K. Jalink and P. Kujala (The Netherlands Cancer Institute) for help with various experiments and the personnel of the experimental animal, flow cytometry and CLSM facilities of the Netherlands Cancer Institute for assistance. This work was supported by grants from the Dutch Cancer Society and The Netherlands Organization for Scientific Research to J.N. and J.B. The authors declare that they have no conflicts of interest.

Supplementary material available online at
http://jcs.biologists.org/cgi/content/full/123/21/3817/DC1

References

Arens, R., Tesselaar, K., van Schijndel, G. M. W., Baars, P. A., Pals, S. T., Krimpenfort, P., Borst, J., van Oers, M. H. J. and van Lier, R. A. W. (2001). Constitutive CD27/CD70 interaction induces expansion of effector-type T cells and results in IFNgamma-mediated B cell depletion. *Immunity* **15**, 801-812.

Bakke, O. and Dobberstein, B. (1990). MHC class II-associated invariant chain contains a sorting signal for endosomal compartments. *Cell* **63**, 707-716.

Banner, D. W., D'Arcy, A., Janes, W., Gentz, R., Schoenfeld, H. J., Broger, C., Loetscher, H. and Lesslauer, W. (1993). Crystal structure of the soluble human 55 kd TNF receptor-human TNF beta complex: implications for TNF receptor activation. *Cell* **73**, 431-445.

Bénaroch, P., Yilla, M., Raposo, G., Ito, K., Miwa, K., Geuze, H. J. and Ploegh, H. L. (1995). How MHC class II molecules reach the endocytic pathway. *EMBO J.* **14**, 37-49.

Bikoff, E. K., Huang, L. Y., Episkopou, V., van Meerwijk, J., Germain, R. N. and Robertson, E. J. (1993). Defective major histocompatibility complex class II assembly, transport, peptide acquisition, and CD4$^+$ T cell selection in mice lacking invariant chain expression. *J. Exp. Med.* **177**, 1699-1712.

Boes, M., Cerny, J., Massol, R., Op den Brouw, M., Kirchhausen, T., Chen, J. and Ploegh, H. (2002). T-cell engagement of dendritic cells rapidly rearranges MHC class II transport. *Nature* **418**, 983-988.

Boes, M., Bertho, N., Cerny, J., Op den Brouw, M., Kirchhausen, T., Ploegh, H. (2003). T cells induce extended class II MHC compartments in dendritic cells in a Toll-like receptor-dependent manner. *J. Immunol.* **171**, 4081-4088.

Bryant, P. W., Roos, P., Ploegh, H. L. and Sant, A. J. (1999). Deviant trafficking of I-A^d mutant molecules is reflected in their peptide binding properties. *Eur. J. Immunol.* **29**, 2729-2739.

Calafat, J., Janssen, H., Stahle-Backdahl, M., Zuurbier, A. E., Knol, E. F. and Egesten, A. (1997). Human monocytes and neutrophils store transforming growth factor-alpha in a subpopulation of cytoplasmic granules. *Blood* **90**, 1255-1266.

Chang, C. H. and Flavell, R. A. (1995). Class II transactivator regulates the expression of multiple genes involved in antigen presentation. *J. Exp. Med.* **181**, 765-767.

Chow, A., Toomre, D., Garrett, W. and Mellman, I. (2002). Dendritic cell maturation triggers retrograde MHC class II transport from lysosomes to the plasma membrane. *Nature* **418**, 988-994.

Cosgrove, D., Gay, D., Dierich, A., Kaufman, J., Lemeur, M., Benoist, C. and Mathis, D. (1991). Mice lacking MHC class II molecules. *Cell* **66**, 1051-1066.

Cresswell, P. (1994). Assembly, transport and function of MHC class II molecules. *Annu. Rev. Immunol.* **12**, 259-293.

de Graaf, P., Zwart, W. T., van Dijken, R. A., Deneka, M., Schultz, T. K., Geijsen, N., Coffer, P. J., Gadella, B. M., Verkleij, A. J., van der Sluijs, P. et al. (2004). Phosphatidylinositol 4-kinase beta is critical for functional association of rab11 with the Golgi complex. *Mol. Biol. Cell* **15**, 2038-2047.

Dugast, M., Toussaint, H., Dousset, C. and Benaroch, P. (2005). AP2 clathrin adaptor complex, but not AP1, controls the access of the major histocompatibility complex (MHC) class II to endosomes. *J. Biol. Chem.* **280**, 19656-19664.

Förster, T. (1948). Zwischemolekulare energiewanderung und fluoreszenz. *Ann. Physik* **2**, 55-67.

Goodwin, R. G., Alderson, M. R., Smith, C. A., Armitage, R. J., Vandenbos, T., Jerzy, R., Tough, T. W., Schoenborn, M., Davies-Smith, T., Hennen, K. et al. (1993). Molecular and biological characterization of a ligand for CD27 defines a new family of cytokines with homology to tumor necrosis factor. *Cell* **73**, 447-456.

Hendriks, J., Xiao, Y. and Borst, J. (2003). CD27 promotes survival of activated T cells and complements CD28 in generation and establishment of the effector T cell pool. *J. Exp. Med.* **198**, 1369-1380.

Hendriks, J., Xiao, Y., Rossen, J. W. A., Van der Sluijs, K. F., Sugamura, K., Ishii, N. and Borst, J. (2005). During viral infection of the respiratory tract, CD27, 4-1BB, and OX40 collectively determine formation of CD8$^+$ memory T cells and their capacity for secondary expansion. *J. Immunol.* **175**, 1665-1676.

Hintzen, R. Q., Lens, S. M., Koopman, G., Pals, S. T., Spits, H. and Van Lier, R. A. (1994). CD70 represents the human ligand for CD27. *Int. Immunol.* **6**, 477-480.

Jasanoff, A., Wagner, G. and Wiley, D. C. (1998). Structure of a trimeric domain of the MHC class II-associated chaperonin and targeting protein Ii. *EMBO J.* **17**, 6812-6818.

Jayawardena-Wolf, J., Benlagha, K., Chiu, Y.-H., Meher, R. and Bendelac, A. (2001). CD1d endosomal trafficking is independently regulated by an intrinsic CD1d-encoded tyrosine motif and by the invariant chain. *Immunity* **15**, 897-908.

Kang, S. J. and Cresswell, P. (2002). Regulation of intracellular trafficking of human CD1d by association with MHC class II molecules. *EMBO J.* **21**, 1650-1660.

Keller, A. M., Groothuis, T. A., Veraar, E. A. M., Marsman, M., Maillette de Buy Wenniger, L., Janssen, H., Neefjes, J. and Borst, J. (2007). Costimulatory ligand CD70 is delivered to the immunological synapse by shared intracellular trafficking with MHC class II molecules. *Proc. Natl. Acad. Sci. USA* **104**, 5989-5994.

Keller, A. M., Schildknecht, A., Xiao, Y., van den Broek, M. and Borst, J. (2008). Expression of costimulatory ligand CD70 on steady-state dendritic cells breaks CD8$^+$ T cell tolerance and permits effective immunity. *Immunity* **29**, 934-946.

Klausner, R. D., Donaldson, J. G. and Lippincott-Schwartz, J. (1992). Brefeldin A: insights into the control of membrane traffic and organelle structure. *J. Cell Biol.* **116**, 1071-1080.

Kleijmeer, M., Ramm, G., Schuurhuis, D., Griffith, J., Rescigno, M., Ricciardi-Castagnoli, P., Rudensky, A. Y., Ossendorp, F., Melief, C. J. M., Stoorvogel, W. et al. (2001). Reorganization of multivesicular bodies regulates MHC class II antigen presentation by dendritic cells. *J. Cell Biol.* **155**, 53-63.

Koch, N., Lauer, W., Habicht, J. and Dobberstein, B. (1987a). Primary structure of the gene for murine Ia antigen-associated invariant chains (Ii). An alternative spliced exon encodes a cysteine-rich domain highly homologous to a repetitive sequence of thyroglobulin. *EMBO J.* **6**, 1677-1683.

Koch, S., Schultz, A. and Koch, N. (1987b). The production of recombinant HLA-DR beta and invariant chain polypeptides by cDNA expression in E. coli. *J. Immunol. Methods.* **103**, 211-220.

Lotteau, V., Teyton, L., Peleraux, A., Nilsson, T., Karlsson, L., Schmid, S. L., Quaranta, V. and Peterson, P. A. (1990). Intracellular transport of class II MHC molecules directed by invariant chain. *Nature* **348**, 600-605.

Machamer, C. E. and Cresswell, P. (1982). Biosynthesis and glycosylation of the invariant chain associated with HLA-DR antigens. *J. Immunol.* **129**, 2564-2569.

Marks, M. S., Blum, J. S. and Cresswell, P. (1990). Invariant chain trimers are sequestered in the rough endoplasmic reticulum in the absence of association with HLA class II antigens. *J. Cell Biol.* **111**, 839-855.

McCormick, P. J., Martina, J. A. and Bonifacino, J. S. (2005). Involvement of clathrin and AP-2 in the trafficking of MHC class II molecules to antigen-presenting compartments. *Proc. Natl. Acad. Sci. USA* **102**, 7910-7915.

Michelsen, K., Yuan, H. and Schwappach, B. (2005). Hide and run. Arginine-based endoplasmatic reticulum-sorting motifs in the assembly of heteromultimeric membrane proteins. *EMBO Rep.* **6**, 717-722.

Morton, P. A., Zacheis, M. L., Giacoletto, K. S., Manning, J. A. and Schwartz, B. D. (1995). Delivery of nascent MHC class Ii-invariant chain complexes to lysosomal compartments and proteolysis of invariant chain by cysteine proteases precedes peptide binding in B-lymphoblastoid cells. *J. Immunol.* **154**, 137-150.

Naik, S. H., Proietto, A. I., Wilson, N. S., Dakic, A., Schnorrer, P., Fuchsberger, M., Lahoud, M. H., O'Keeffe, M., Shao, Q. X., Chen, W. F. et al. (2005). Cutting edge: generation of splenic CD8+ and CD8- dendritic cell equivalents in Fms-like tyrosine kinase 3 ligand bone marrow cultures. *J. Immunol.* **174**, 6592-6597.

Nakamura, N., Lowe, M., Levine, T. P., Rabouille, C. and Warren, G. (1997). The vesicle docking protein p115 binds GM130, a *cis*-Golgi matrix protein, in a mitotically regulated manner. *Cell* **89**, 445-455.

Neefjes, J. J. and Ploegh, H. L. (1992). Inhibition of endosomal proteolytic activity by leupeptin blocks surface expression of MHC class II molecules and their conversion to SDS resistance alpha beta heterodimers in endosomes. *EMBO J.* **11**, 411-416.

Neefjes, J. J., Stollorz, V., Peters, P. J., Geuze, H. J. and Ploegh, H. L. (1990). The biosynthetic pathway of MHC class II but not class I molecules intersects the endocytic route. *Cell* **61**, 171-183.

Nijenhuis, M. and Neefjes, J. (1994). Early events in the assembly of major histocompatibility complex class II heterotrimers from their free subunits. *Eur. J. Immunol.* **24**, 247-256.

O'Sullivan, D. M., Noonan, D. and Quaranta, V. (1987). Four Ia invariant chain forms derive from a single gene by alternate splicing and alternate initiation of transcription/translation. *J. Exp. Med.* **166**, 444-460.

Odorizzi, G. C., Trowbridge, I. S., Xue, L., Hopkins, C. R., Davis, C. D. and Collawn, J. F. (1994). Sorting signals in the MHC class II invariant chain cytoplasmic tail and transmembrane region determine trafficking to an endocytic processing compartment. *J. Cell Biol.* **126**, 317-330.

Oshima, H., Nakano, H., Nohara, C., Kobata, T., Nakajima, A., Jenkins, N. A., Gilbert, D. J., Copeland, N. G., Muto, T., Yagita, H. et al. (1998). Characterization of murine CD70 by molecular cloning and mAb. *Int. Immunol.* **10**, 517-526.

Peters, P. J., Neefjes, J. J., Oorschot, V., Ploegh, H. L. and Geuze, H. J. (1991). Segregation of MHC class II molecules from MHC class I molecules in the Golgi complex for transport to lysosomal compartments. *Nature* **349**, 669-676.

Peters, P. J., Raposo, G., Neefjes, J. J., Oorschot, V., Leijendekker, R. L., Geuze, H. J. and Ploegh, H. L. (1995). Major histocompatibility complex class II compartments in human B lymphoblastoid cells are distinct from early endosomes. *J. Exp. Med.* **182**, 325-334.

Pieters, J., Horstmann, H., Bakke, O., Griffiths, G. and Lipp, J. (1991). Intracellular transport and localization of major histocompatibility complex class II molecules and associated invariant chain. *J. Cell Biol.* **115**, 1213-1223.

Rocha, N. and Neefjes, J. (2008). MHC Class II molecules on the move for successful antigen presentation. *EMBO J.* **27**, 1-5.

Romagnoli, P., Layet, C., Yewdell, J., Bakke, O., Germain, R. N. (1993). Relationship between invariant chain expression and major histocompatibility complex class II transport into early and late endocytic compartments. *J. Exp. Med.* **177**, 583-596.

Sanchez, P. J., McWilliams, J. A., Haluszczak, C., Yagita, H. and Kedl, R. M. (2007). Combined TLR/CD40 stimulation mediates potent cellular immunity by regulating dendritic cell expression of CD70 in vivo. *J. Immunol.* **178**, 1564-1572.

Soares, H., Waechter, H., Glaichenhaus, N., Mougneau, E., Yagita, H., Mizenina, O., Dudziak, D., Nussenzweig, M. C. and Steinman, R. M. (2007). A subset of dendritic cells induces CD4+ T cells to produce IFN-γ by an IL-12-independent but CD70-dependent mechanism in vivo. *J. Exp. Med.* **204**, 1095-1106.

Steinman, R. M., Hawiger, D. and Nussenzweig, M. C. (2003). Tolerogenic dendritic cells. *Annu. Rev. Immunol.* **21**, 685-711.

Strubin, M., Berte, C. and Mach, B. (1986). Alternative splicing and alternative initiation of translation explain the four isoforms of the Ia antigen-associated invariant chain. *EMBO J.* **5**, 3483-3488.

Tesselaar, K., Gravestein, L. A., van Schijndel, G. M., Borst, J. and van Lier, R. A. (1997). Characterization of murine CD70, the ligand of the TNF receptor family member CD27. *J. Immunol.* **159**, 4959-4965.

Tesselaar, K., Arens, R., van Schijndel, G. M. W., Baars, P. A., van der Valk, M., Borst, J., van Oers, M. H. J. and van Lier, R. A. W. (2003a). Lethal T cell immunodeficiency induced by chronic costimulation via CD27-CD70 interactions. *Nat. Immunol.* **4**, 49-54.

Tesselaar, K., Xiao, Y., Arens, R., van Schijndel, G. M. W., Schuurhuis, D. H., Mebius, R., Borst, J. and van Lier, R. A. W. (2003b). Expression of the murine CD27 ligand CD70 in vitro and in vivo. *J. Immunol.* **170**, 33-40.

van Niel, G., Wubbolts, R., Ten Broeke, T., Buschow, S. I., Ossendorp, F. A., Melief, C. J., Raposo, G., van Balkom, B. W. and Stoorvogel, W. (2006). Dendritic cells regulate exposure of MHC class II at their plasma membrane by oligoubiquitination. *Immunity* **25**, 885-894.

van Rheenen, J., Langeslag, M. and Jalink, K. (2004). Correcting confocal acquisition to optimize imaging of fluorescence resonance energy transfer by sensitized emission. *Biophys. J.* **86**, 2517-2529.

Villadangos, J. A., Cardoso, M., Steptoe, R. J., van Berkel, D., Pooley, J., Carbone, F. R. and Shortman, K. (2001). MHC class II expression is regulated in dendritic cells independently of invariant chain degradation. *Immunity* **14**, 739-744.

Viville, S., Neefjes, J., Lotteau, V., Dierich, A., Lemeur, M., Ploegh, H., Benoist, C. and Mathis, D. (1993). Mice lacking the MHC class II-associated invariant chain. *Cell* **72**, 635-648.

Vyas, J. M., Kim, Y. M., Artavanis-Tsakonas, K., Love, J. C., Van der Veen. A. G. and Ploegh, H. L. (2007). Tubulation of class II MHC compartments is microtubule dependent and involves multiple endolysosomal membrane proteins in primary dendritic cells. *J. Immunol.* **178**, 7199-7210.

Wubbolts, R. W., Fernandez-Borja, M., Oomen, L., Verwoerd, D., Janssen, H., Calafat, J., Tulp, A., Dusseljee, S. and Neefjes, J. (1996). Direct vesicular transport of MHC class II molecules from lysosomal structures to the cell surface. *J. Cell Biol.* **135**, 611-622.

Xiao, Y., Peperzak, V., Keller, A. M. and Borst, J. (2008). CD27 instructs $CD4^+$ T cells to provide help for the memory $CD8^+$ T cell response after protein immunization. *J. Immunol.* **181**, 1071-1082.

Ye, L., Liu, X., Rout, S. N., Li, Z., Yan, Y., Lu, L., Kamala, T., Nanda, N. K., Song, W., Samal, S. K. et al. (2008). The MHC Class II-associated invariant chain interacts with the neonatal Fcγ receptor and modulates its trafficking to endosomal/lysosomal compartments. *J. Immunol.* **181**, 2572-2585.

Zwart, W., Griekspoor, A., Kuijl, C., Marsman, M., van Rheenen, J., Janssen, H., Calafat, J., van Ham, M., Janssen, L., van Lith, M. et al. (2005). Spatial separation of HLA-DM/HLA-DR interactions within MIIC and phagosome-induced immune escape. *Immunity* **2**, 221-233.

Journal of Cell Science

Table S1. Amino acids sequences of human and mouse Ii isoforms. In this study, we have used a cDNA construct encoding the p33 isoform of human Ii that ordinarily arises from p35 (isoform 2b, NCBI) mRNA by the use of an alternative translational start site. The start methionine of p33 is indicated in bold. In p33, the arginine-rich amino-terminal sequence (underlined) is lacking that contains an ER retention motif. In human p43 and mouse p41 the additional sequence that is encoded by exon 6b and discriminates them from p35 and p31 respectively, is underlined. The transmembrane domain is highlighted in each Ii protein. All depicted Ii species have the lysosomal targeting motifs. Literature references to cited information are given in the manuscript text.

Human Ii isoform a (p43)

```
                                                                TM
1 mhrrrsrscr edqkpvmddq rdlisnneql pmlgrrpgap eskcsrgaly tgfsilvtll
       61 lagqattayf lyqqqgrldk ltvtsqnlql enlrmklpkp pkpvskmrma tpllmqalpm
      121 galpqgpmqn atkygnmted hvmhllqnad plkvypplkg sfpenlrhlk ntmetidwkv
      181 feswmhhwll femsrhsleq kptdappkvl tkcqeevshi pavhpgsfrp kcdengnylp
      241 lqcygsigyc wcvfpngtev pntrsrghhn csesleledp ssglgvtkqd lgpvpm
```

Human Ii isoform b (p35)

```
                    Start p33
1 mhrrrsrscr edqkpvmddq rdlisnneql pmlgrrpgap eskcsrgaly tgfsilvtll
       61 lagqattayf lyqqqgrldk ltvtsqnlql enlrmklpkp pkpvskmrma tpllmqalpm
      121 galpqgpmqn atkygnmted hvmhllqnad plkvypplkg sfpenlrhlk ntmetidwkv
      181 feswmhhwll femsrhsleq kptdappkes leledpssgl gvtkqdlgpv pm
```

Mouse Ii isoform 1 (p41)

```
1 mddqrdlisn heqlpilgnr prepercsrg alytgvsvlv alllagqatt ayflyqqqgr
       61 ldkltitsqn lqleslrmkl pksakpvsqm rmatpllmrp msmdnmllgp vknvtkygnm
      121 tqdhvmhllt rsgpleypql kgtfpenlkh lknsmdgvnw kifeswmkqw llfemsknsl
      181 eekkpteapp kvltkcqeev shipavypga frpkcdengn ylplqchgst gycwcvfpng
      241 tevphtksrg rhncsepldm edlssglgvt rqelgqvtl
```

Mouse isoform 1 (p31)

```
1 mddqrdlisn heqlpilgnr prepercsrg alytgvsvlv alllagqatt ayflyqqqgr
       61 ldkltitsqn lqleslrmkl pksakpvsqm rmatpllmrp msmdnmllgp vknvtkygnm
      121 tqdhvmhllt rsgpleypql kgtfpenlkh lknsmdgvnw kifeswmkqw llfemsknsl
      181 eekkpteapp kepldmedls sglgvtrqel gqvtl
```